Detector calibration in the JUNO experiment

Akira Takenaka
on behalf of the JUNO collaboration
(Tsung-Dao Lee Institute, Shanghai Jiao Tong University)

NuFact 2024 19th/Sep./2024

JUNO Experiment

PPNP 123, 103927 (2022)

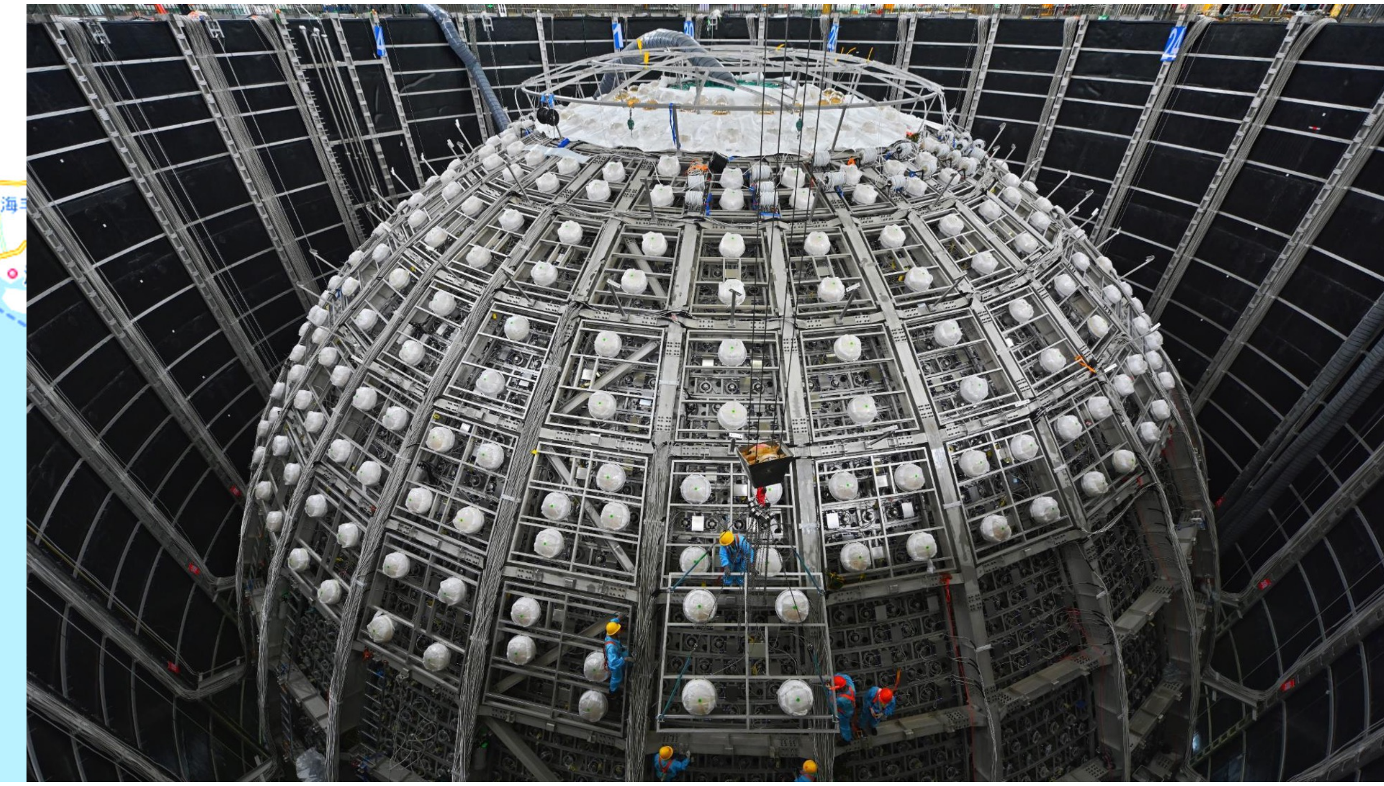

- JUNO will be the world's largest underground (~650 m overburden) liquid scintillator experiment, located in Jiangmen, China.
- The detector is currently under construction and scheduled to begin operations next year.
- The collaboration consists of 74 institutions and over 700 members.

JUNO Plenary Talk: 20th 4:15 PM (Davide Basilico)

JUNO Physics Programs

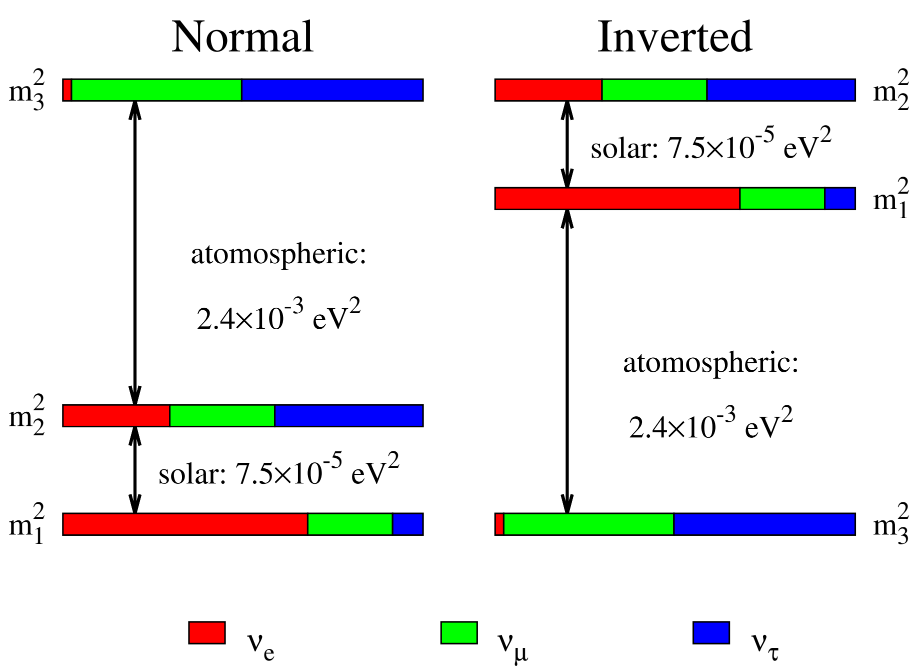

Neutrino mass ordering

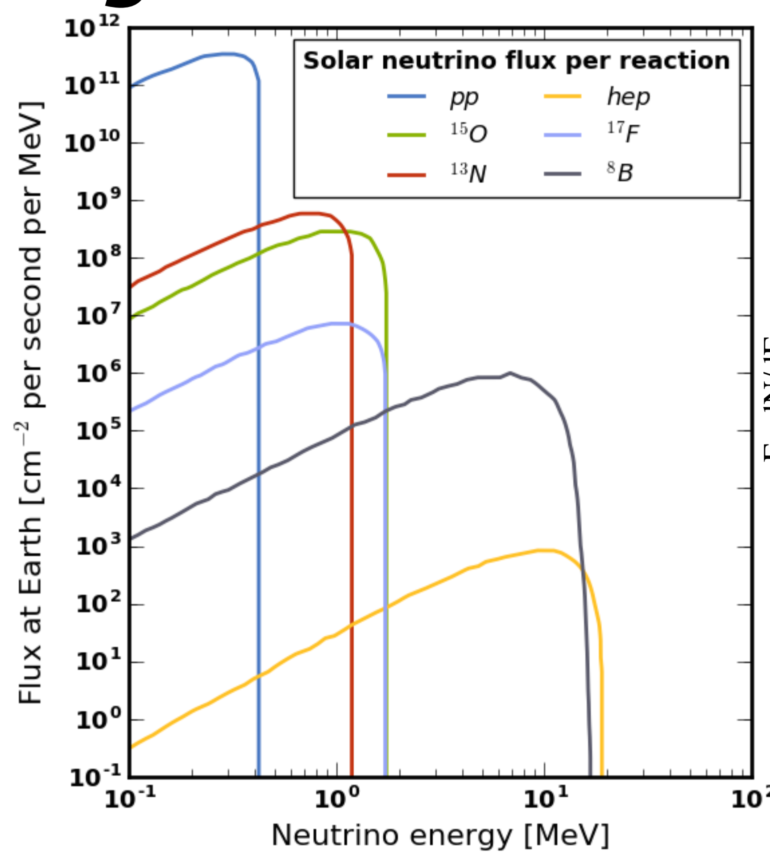

Solar neutrino spectra

PPNP 123, 103927 (2022)

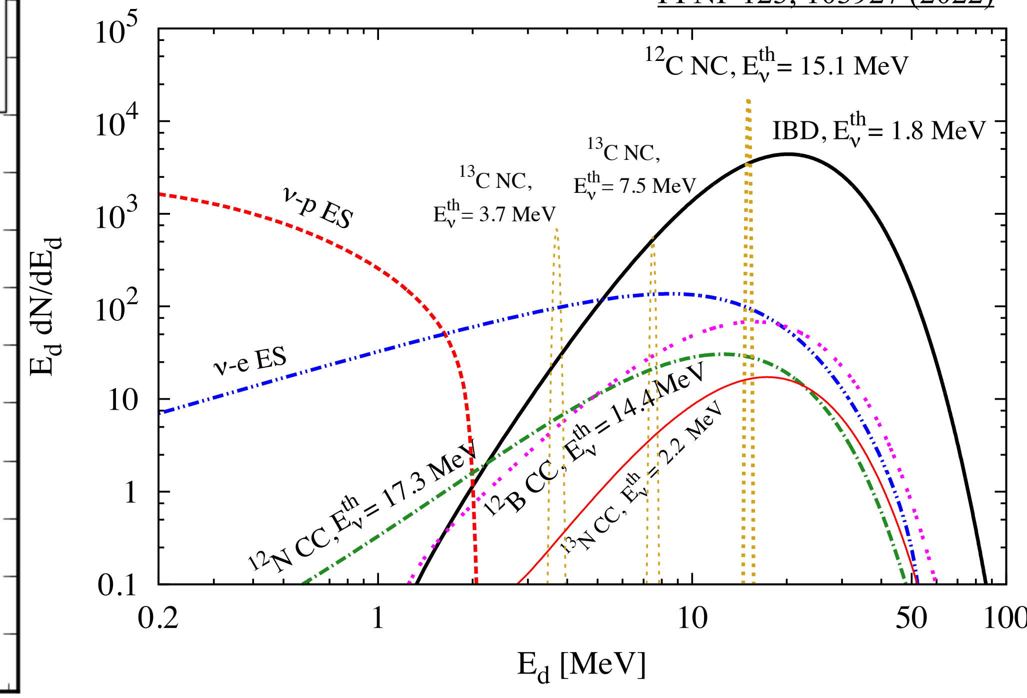

Expected spectra from SN

- JUNO will address a variety of physics topics:
  - Reactor, atmospheric, solar, geo, and supernova neutrino observations,
  - Nucleon decay searches,
  - Other new physics searches, etc.

JUNO Physics Talks: 17th 2:05 PM (Sindhujha Kumaran) and 20th 1:45 PM (Iwan Morton-Blake)

Neutrino Mass Ordering

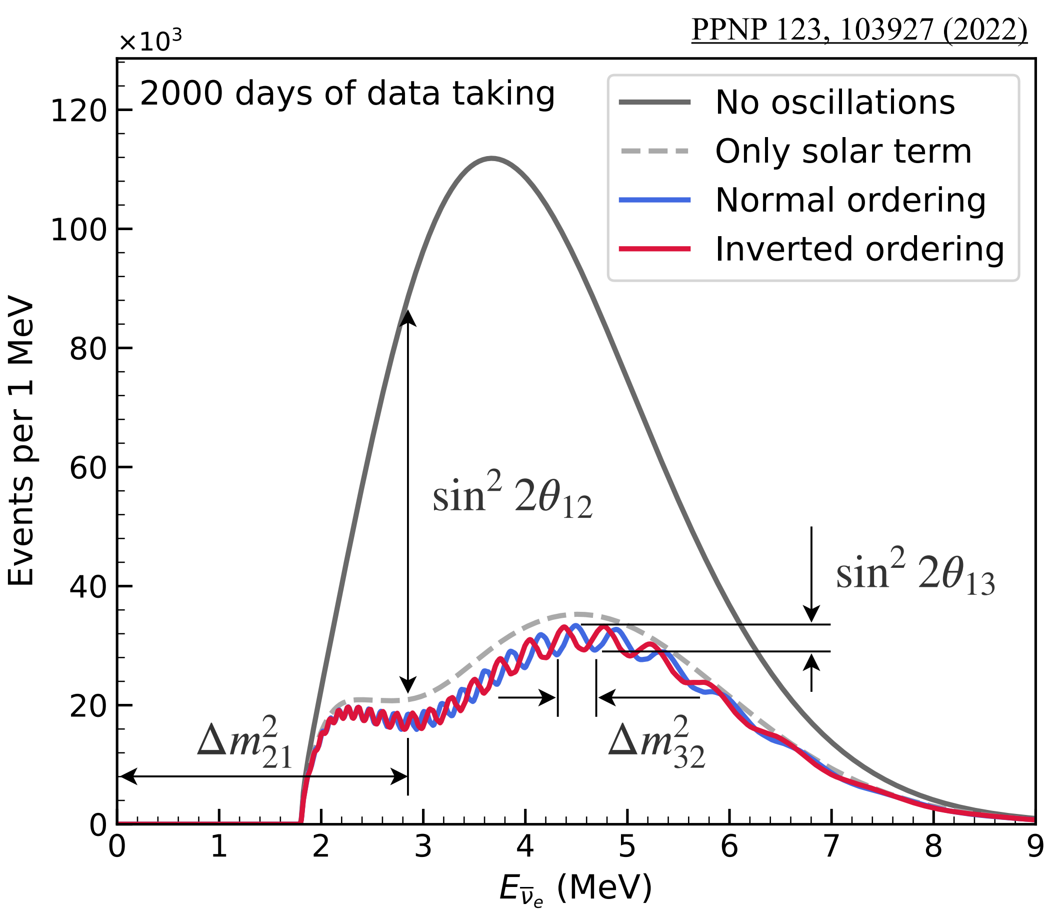

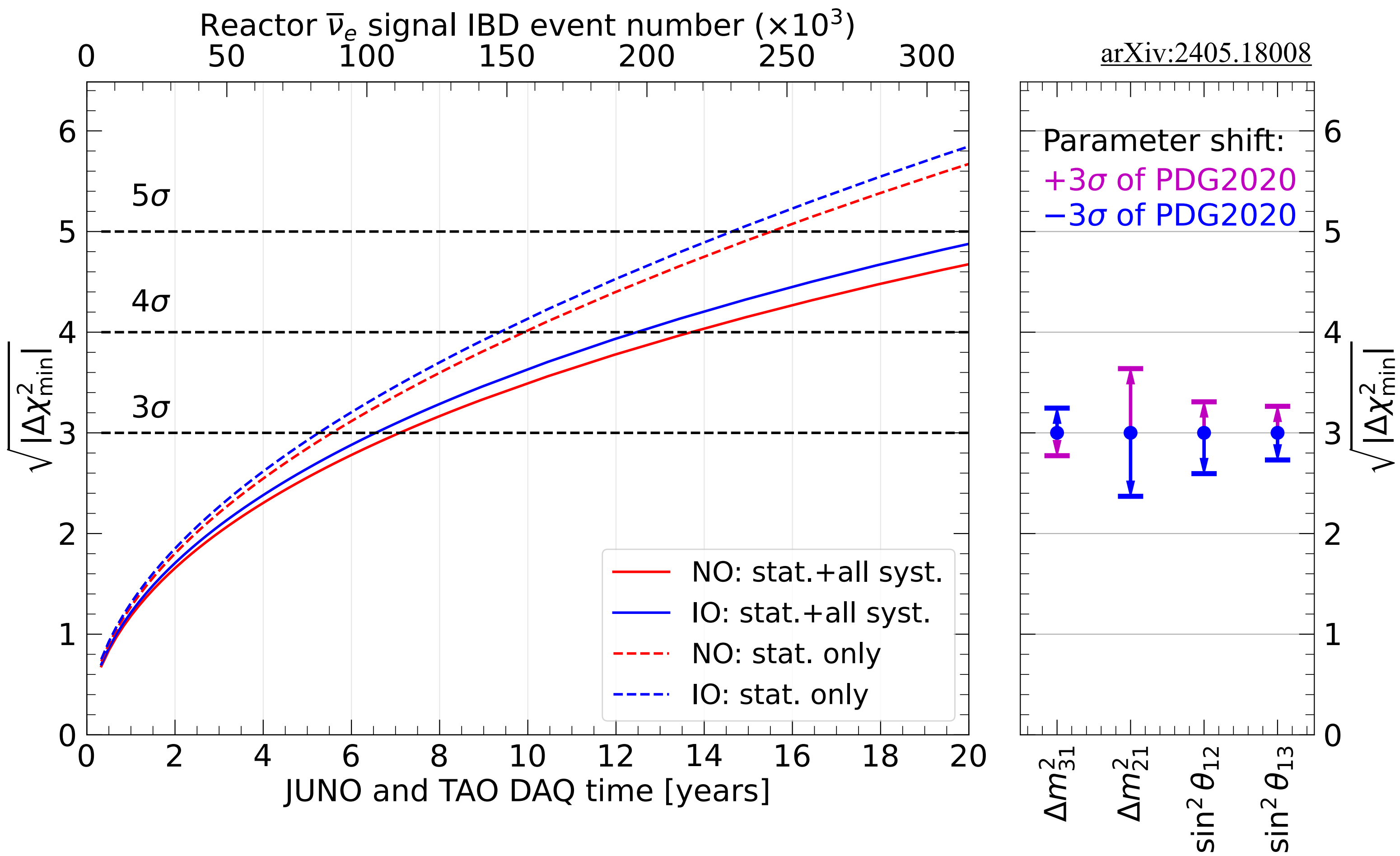

- The primary goal is to determine the neutrino mass ordering from the energy spectrum of reactor neutrinos.
  - The sign of the mass ordering manifests as a phase shift.
- The sensitivity will reach 3σ after ~6 years of operation, assuming:
  - an optimized energy resolution of 3% at 1 MeV.
  - energy scale uncertainty remains below 1%.

JUNO Detector (1)

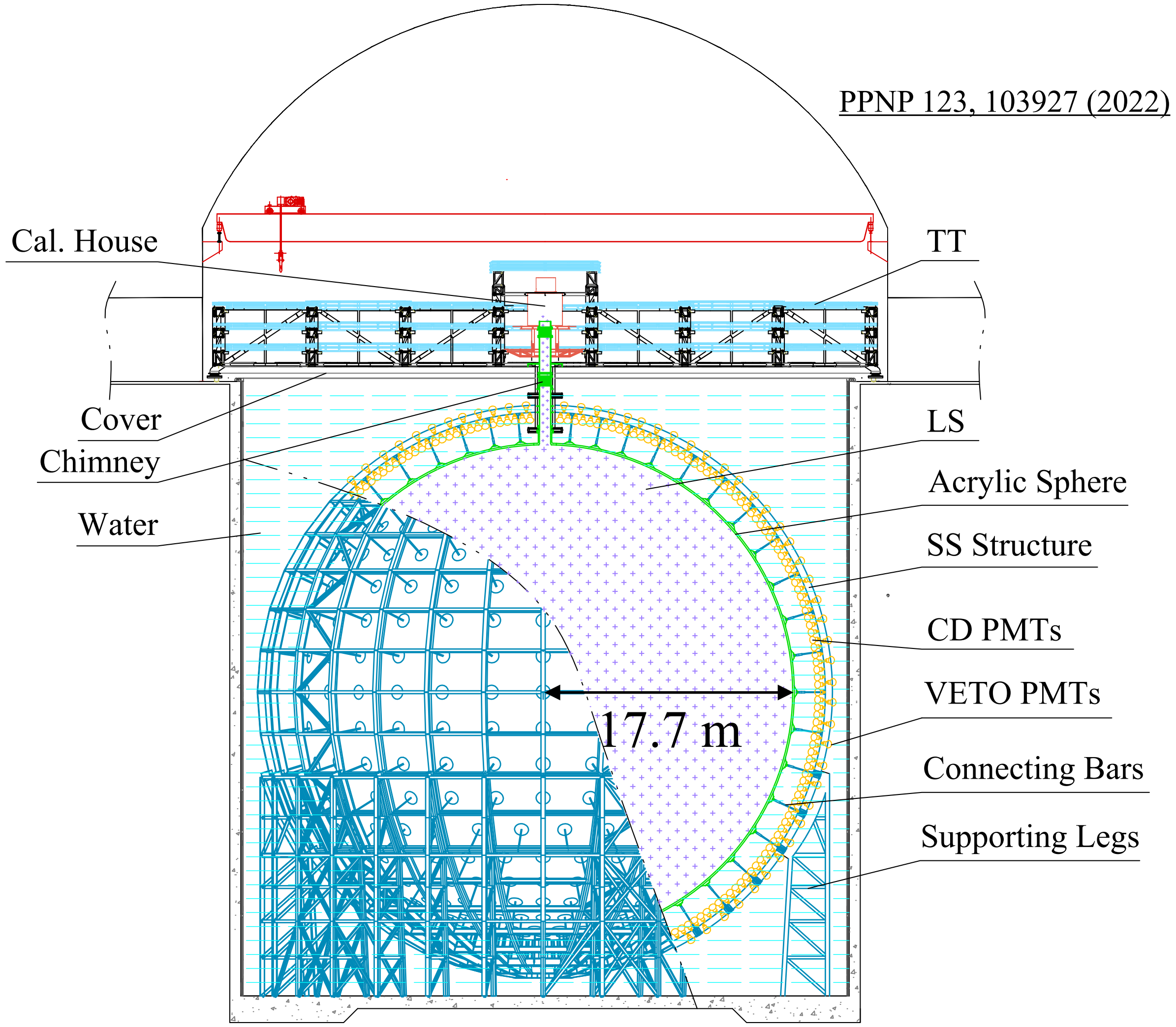

- The 20-kton liquid scintillator (LS) is housed in an acrylic sphere, sustained by a stainless steel structure, submerged in pure water.
    - The composition of the fluor and wavelength shifter in the LS has been optimized to maximize its light yield. NIMA 988, 164823 (2021)

JUNO Detector Talk: 19th 4:55 PM (Marco Beretta), Muon Reconstruction Poster: 16th 4:05 PM (Zekun Yang)

JUNO Detector (2)

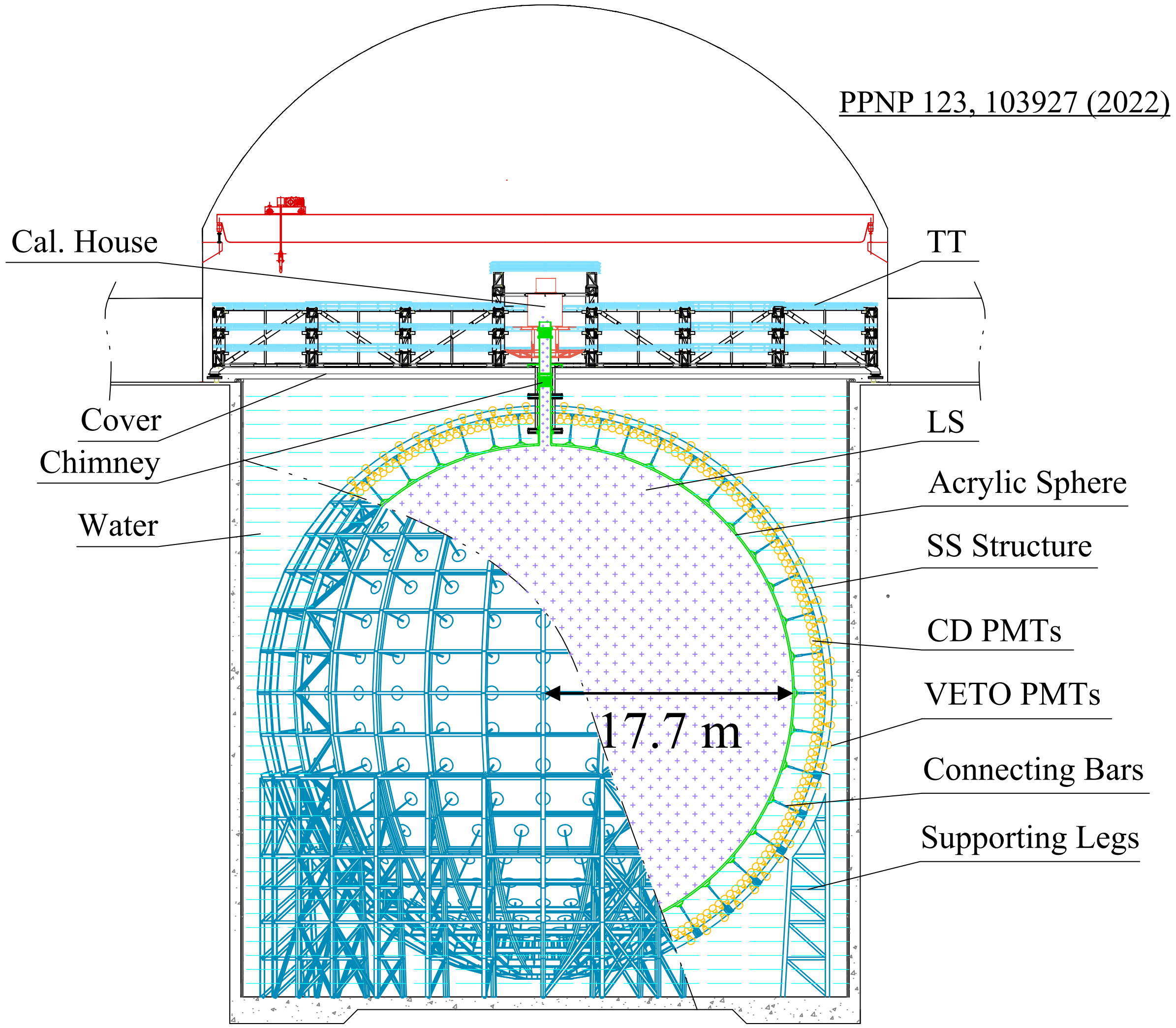

- A large number of photomultiplier tubes (PMTs) are being installed in the stainless steel structure:
  - 17,612 20-inch PMTs, and 25,600 3-inch PMTs.
- The expected number of observed photoelectrons (p.e.) per MeV for events at the detector center is ~1650 p.e.

JUNO Calibration Strategy (1)

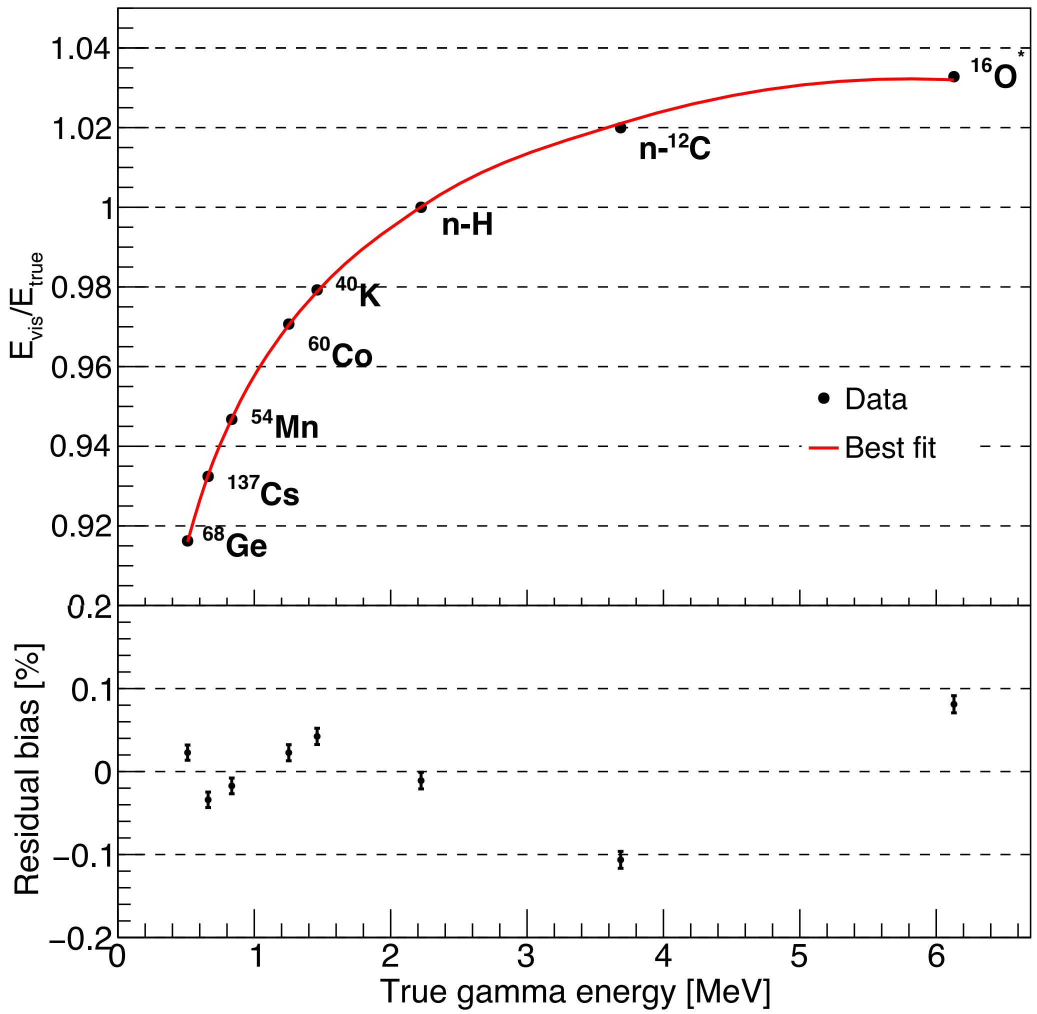

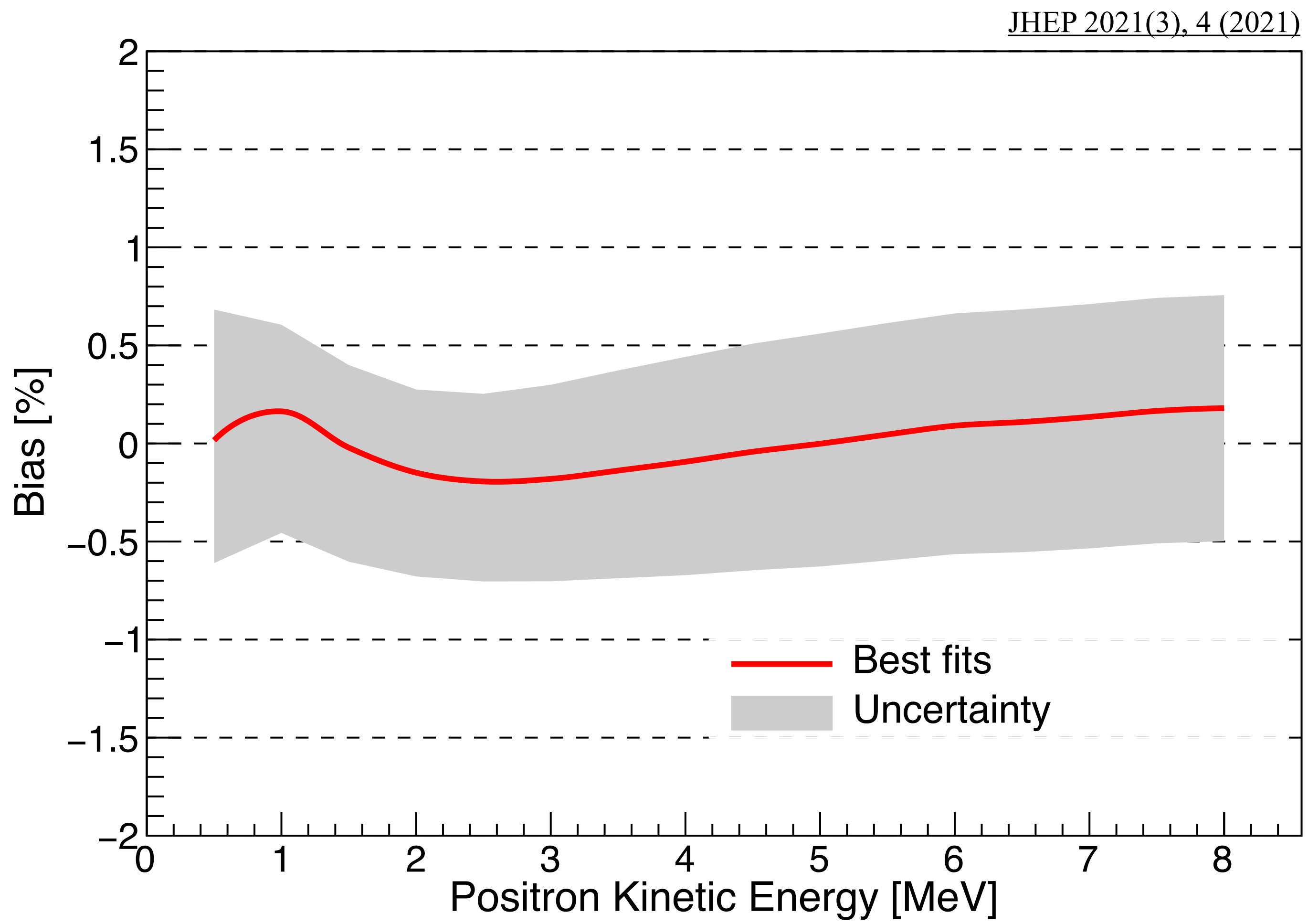

- The light yield of the LS is non-linear to the deposited energy of the particle due to the LS quenching and Cherenkov light contribution.
- Several γ-ray calibration sources will be deployed in the detector to understand this non-linearity and establish a positron energy model.
- In addition, cosmogenic products, such as ^{12}B (Q-value 13.4 MeV), will cover the higher energy region.

JUNO Calibration Strategy (2)

Observed photoelectrons per unit energy w.r.t. the center

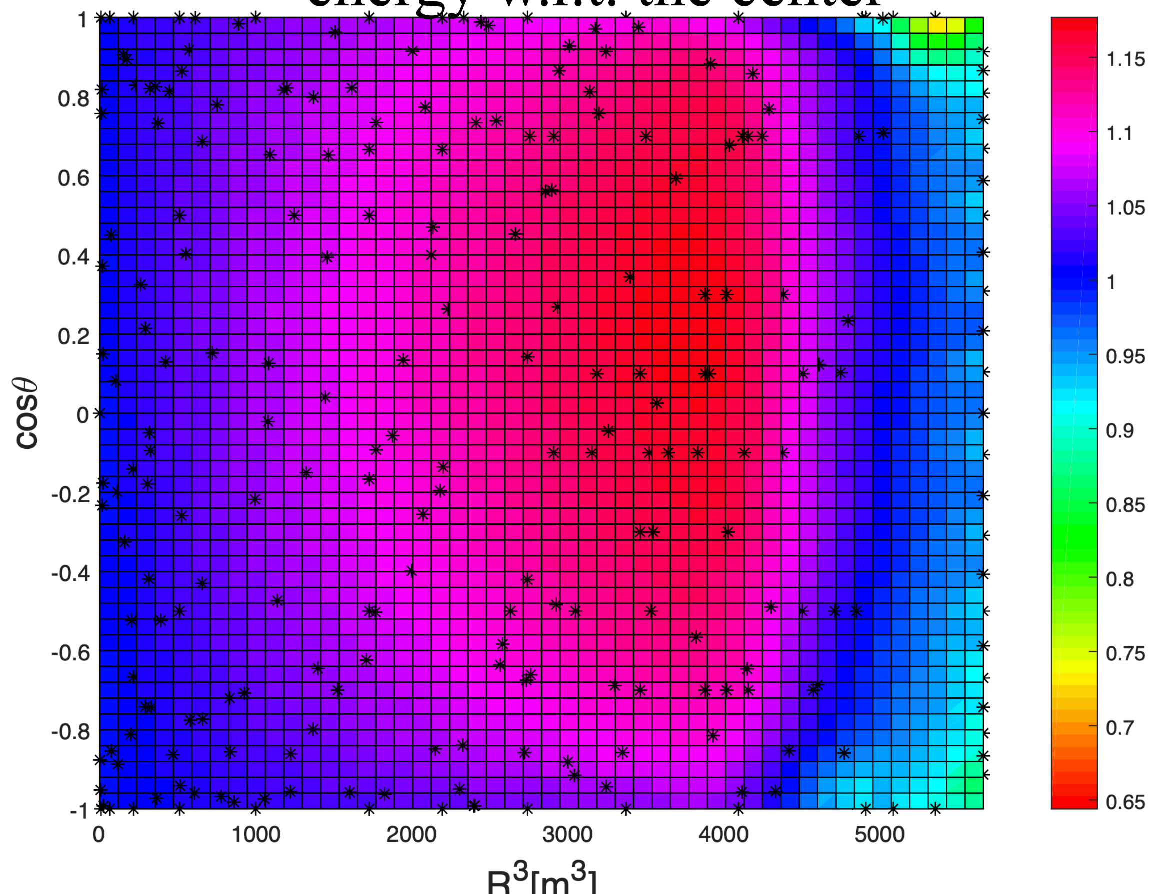

Source deployment positions

JHEP 2021(3), 4 (2021)

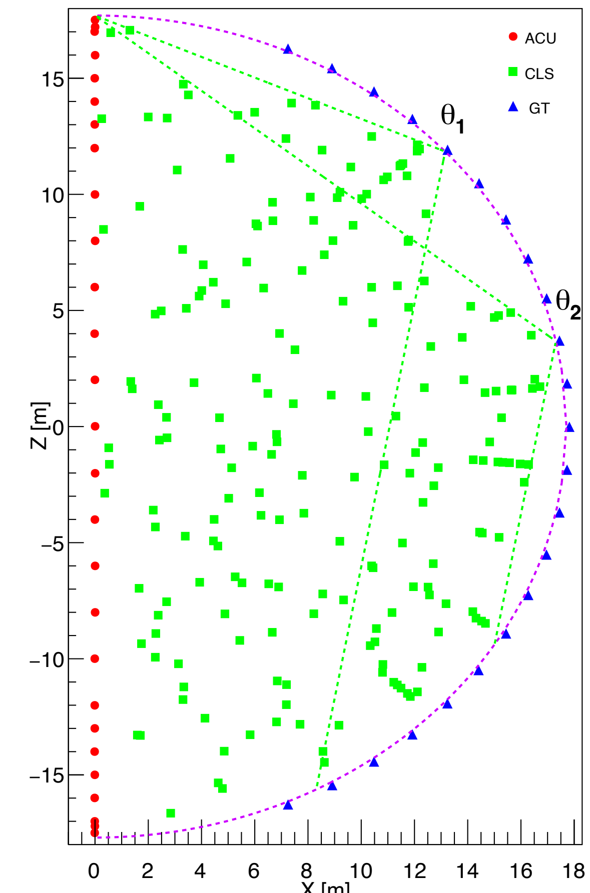

- The observed amount of photoelectrons per unit energy varies more than ±10% due to complex light propagation processes inside the detector, degrading the energy resolution unless corrected.
- This non-uniform energy scale will be calibrated by deploying the calibration source at multiple positions.
- Cosmogenic products, ex. 2.2 MeV γ-ray from spallation neutrons, can also be used to calibrate this.

JUNO Calibration Strategy (3)

JHEP 2021(3), 4 (2021)

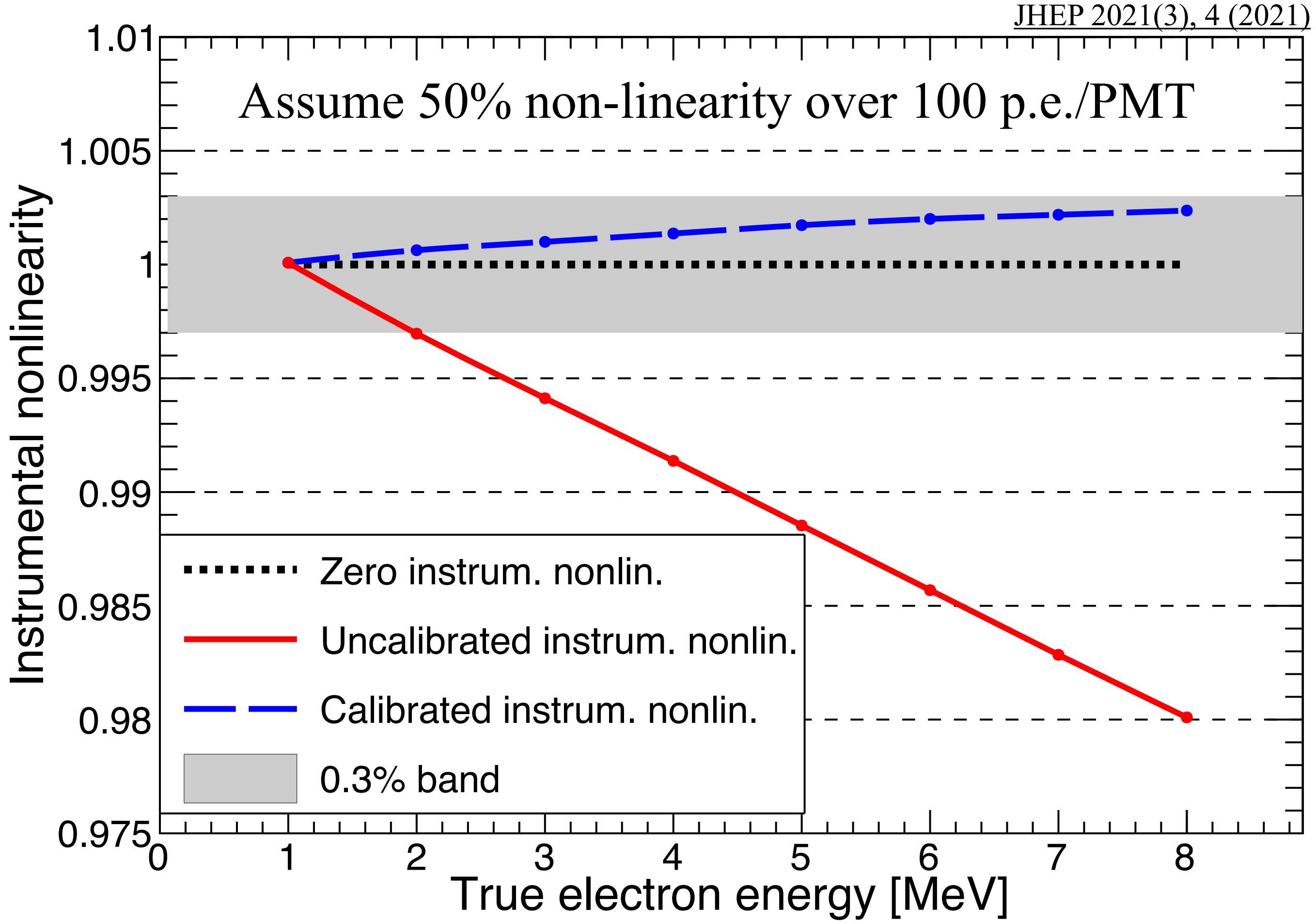

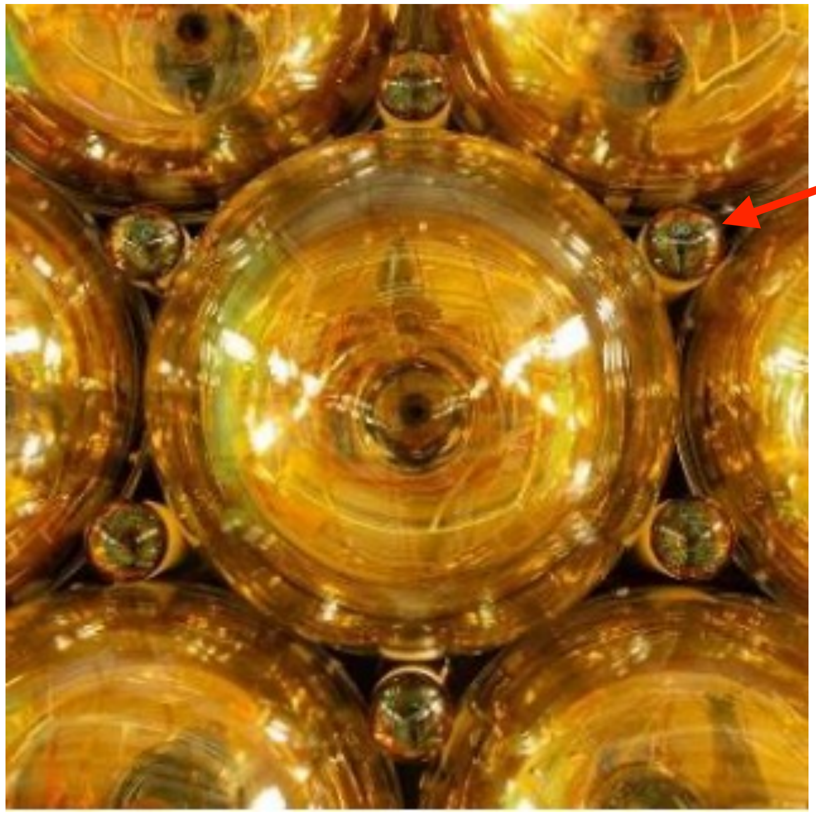

- An inaccurate understanding of the 20-inch PMT non-linearity may degrade the LS non-linearity and non-uniformity calibration qualities.
- A laser calibration source will be used to illuminate the 20-inch PMTs (charge mode) from a single photoelectron to more than 100 p.e.
- By comparing their response to the 3-inch PMTs (mostly single photoelectron counting), this instrumental non-linearity can be calibrated.

JUNO Calibration System

- Multiple calibration source deployment devices will be installed, placing a calibration source at different positions:
  - Automatic Calibration Unit (ACU) will cover the central axis.
  - Cable Loop System (CLS) can cover the off-axis region in a two-dimensional plane.
  - Guide Tube Calibration System (GTCS) will deploy the source on the outer surface of the acrylic sphere.
  - Remotely Operated Vehicle (ROV) can access any position inside the LS volume.

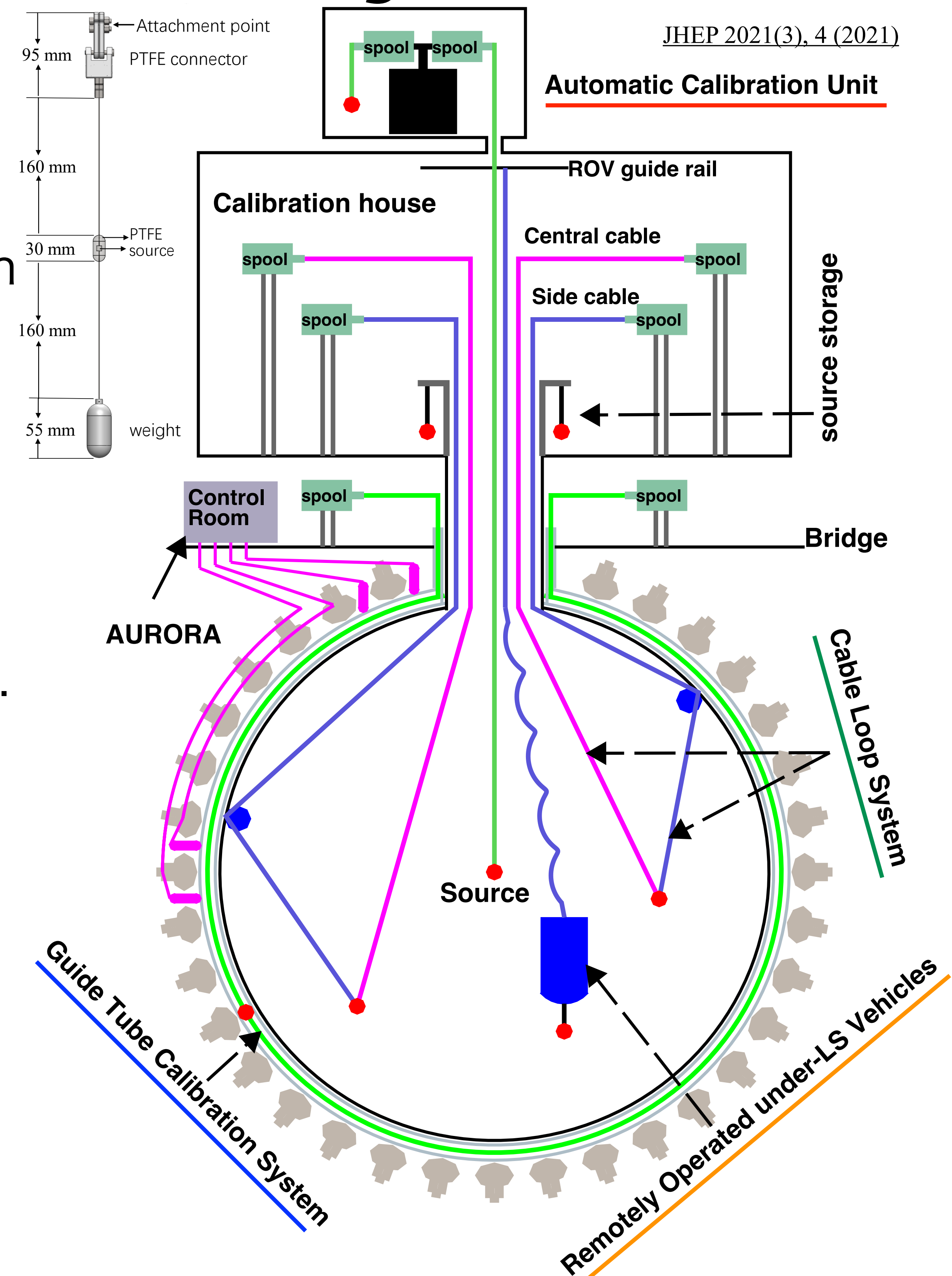

ACU & CLS

- ACU can deploy radioactive and laser sources along the central axis by tuning the wire length with a spool system.
- Position accuracy is estimated to be ~1 cm.
- CLS will move a radioactive source within a two-dimensional plane by adjusting the length of the two wires.
- The source position will be monitored by an ultrasonic system, with ~3 cm accuracy.

JHEP 2021(3), 4 (2021)

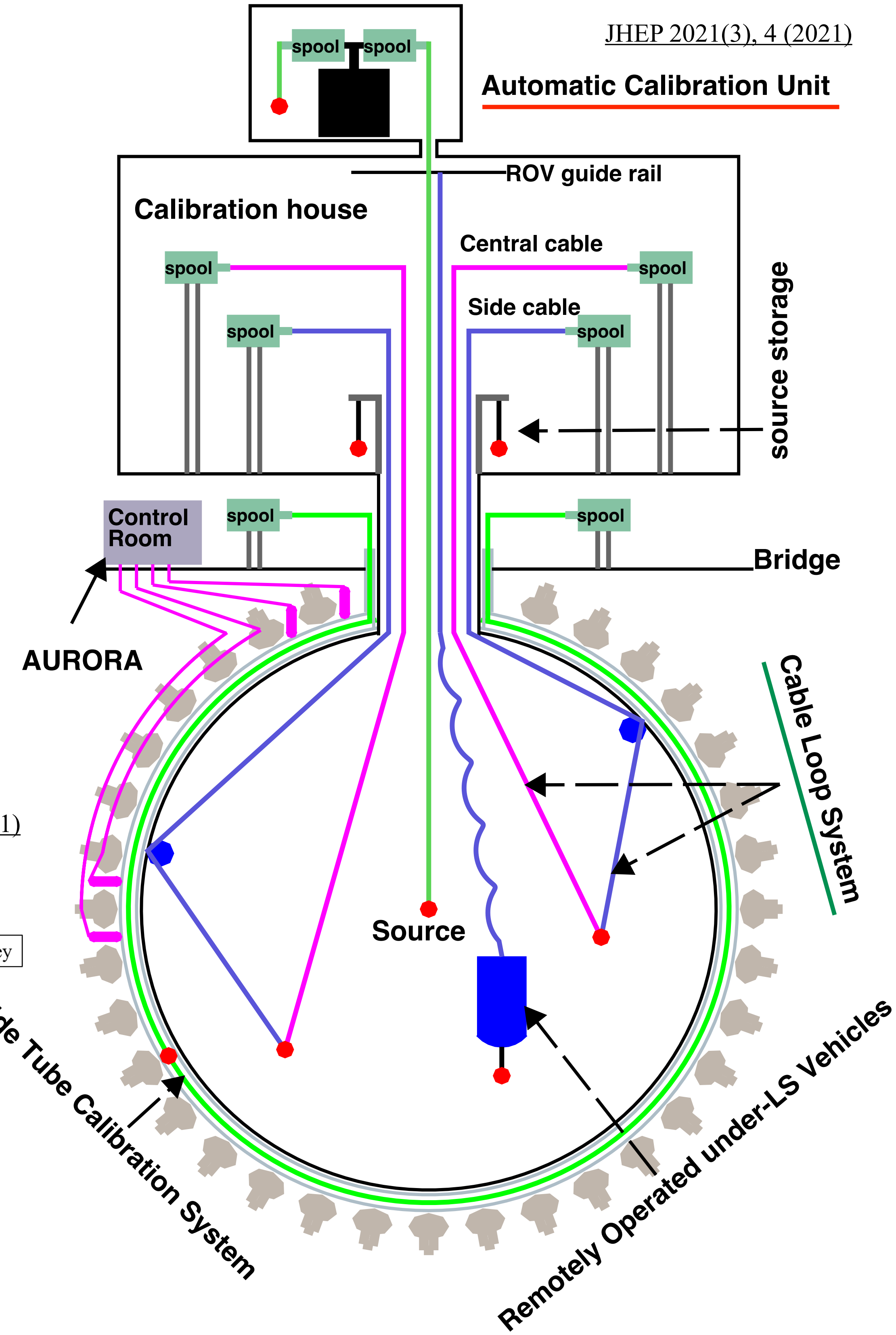

JINST 16(8), T08008 (2021)

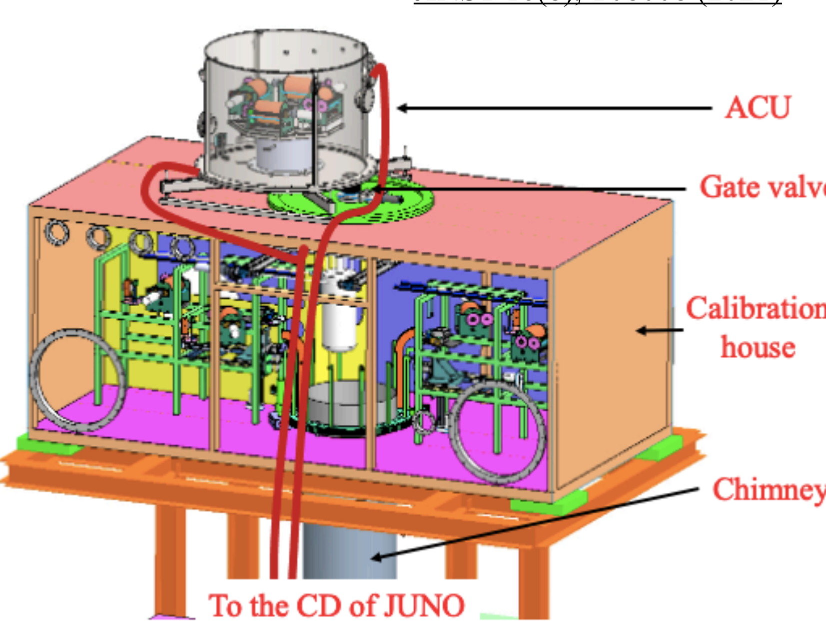

NIMA 988, 164867 (2021)

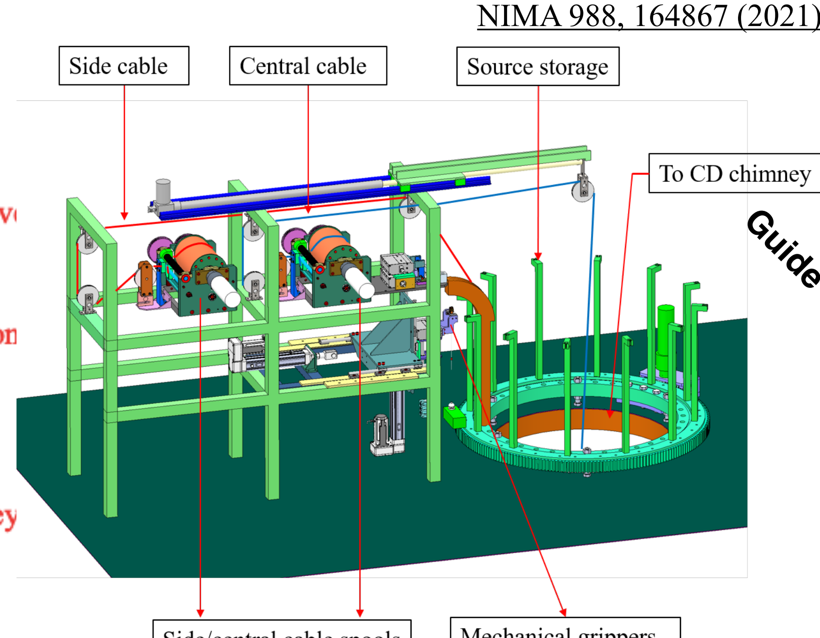

Laser Calibration System

- A laser device placed outside the detector will deliver ultraviolet (UV, λ~267 nm) photons into the LS volume.
  - A light diffuser ball will be placed by ACU.
- UV photons will be absorbed in the LS and visible light will be emitted.
- Using an optical filter, the light intensity can be tuned over a range of more than 4 orders of magnitude to cover the 20-inch PMT dynamic range.

JINST 14(1), P01009 (2019)

UV Laser Device

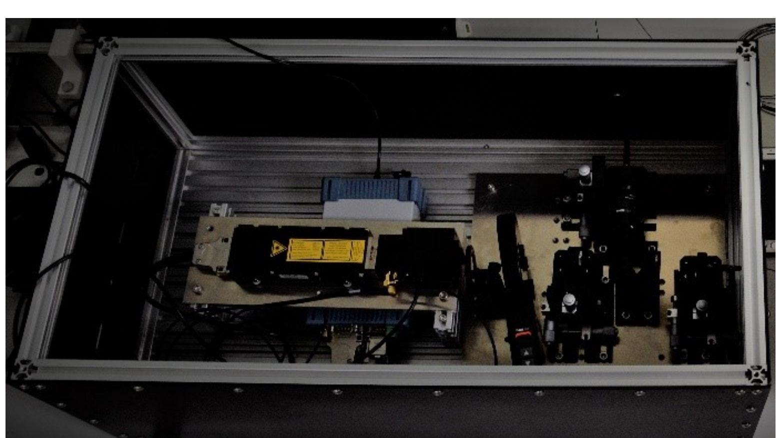

Light Intensity vs. Filter Position

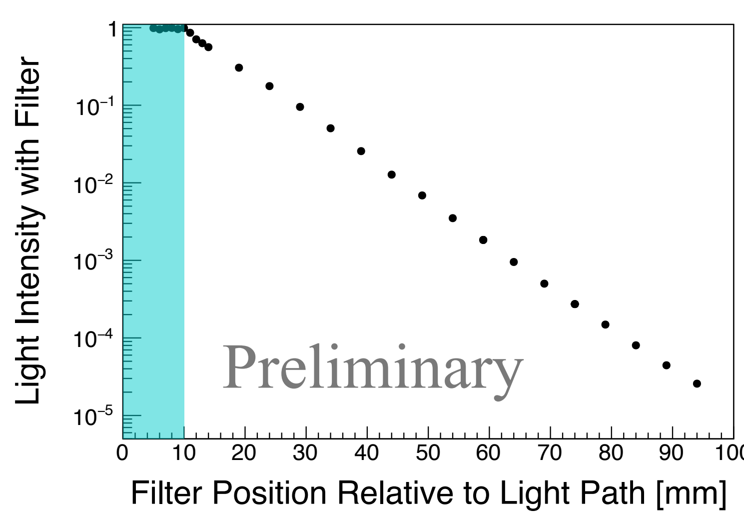

JHEP 2021(3), 4 (2021)

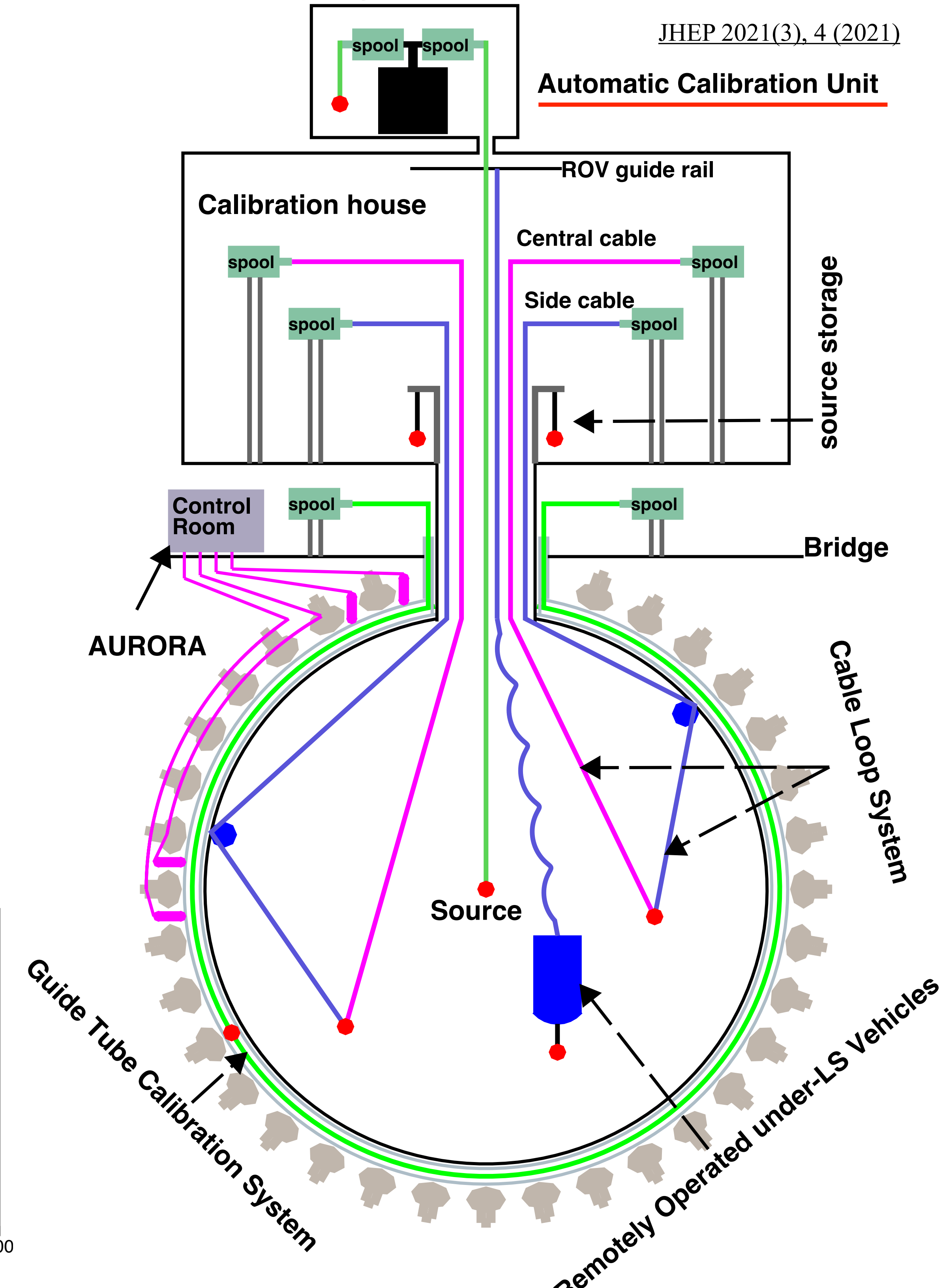

GTCS & ROV

- GTCS will help to calibrate the detector response at the detector edges.
- The source will be moved through the tube attached to the acrylic surface.
- ROV is a submarine deploying a radioactive source.
- Enables to carry out a 3D calibration.

Guide Tubes attached on the acrylic

ROV Testing

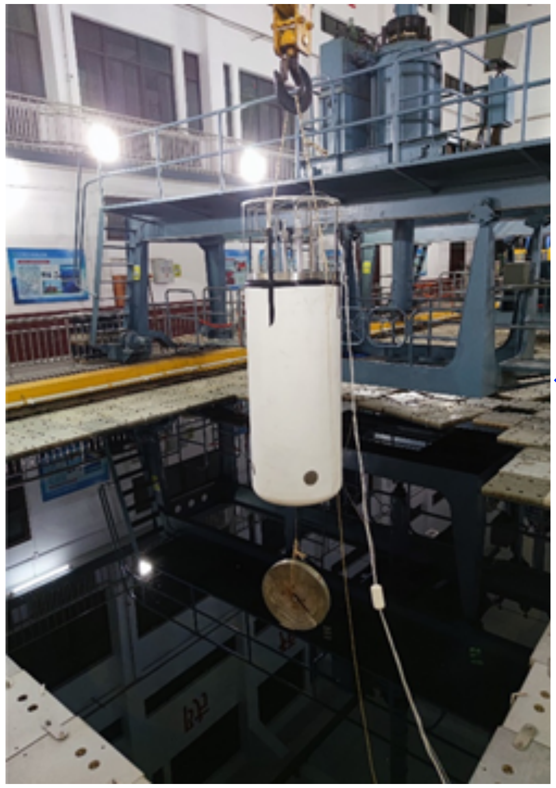

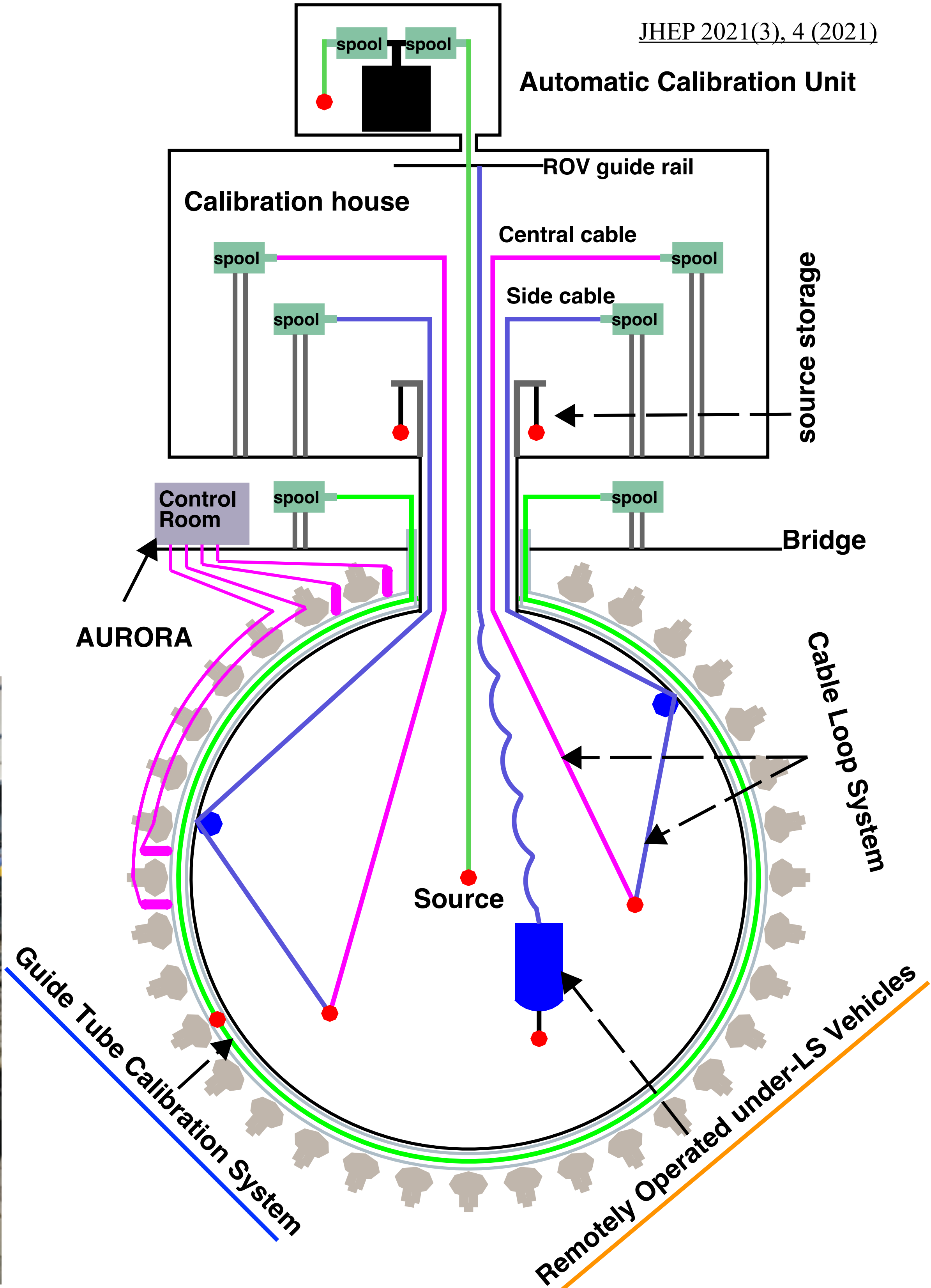

New Calibration Sources (1)

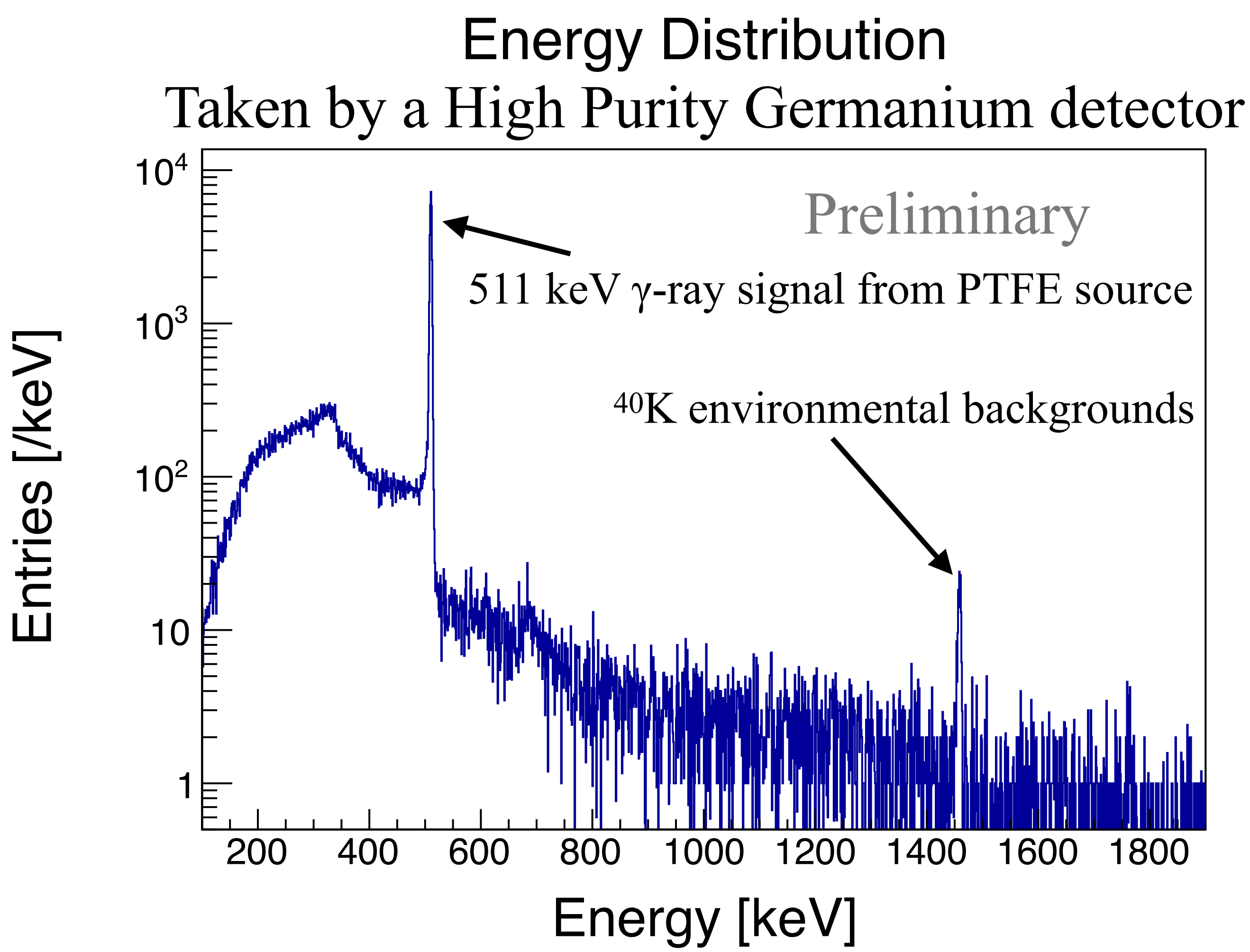

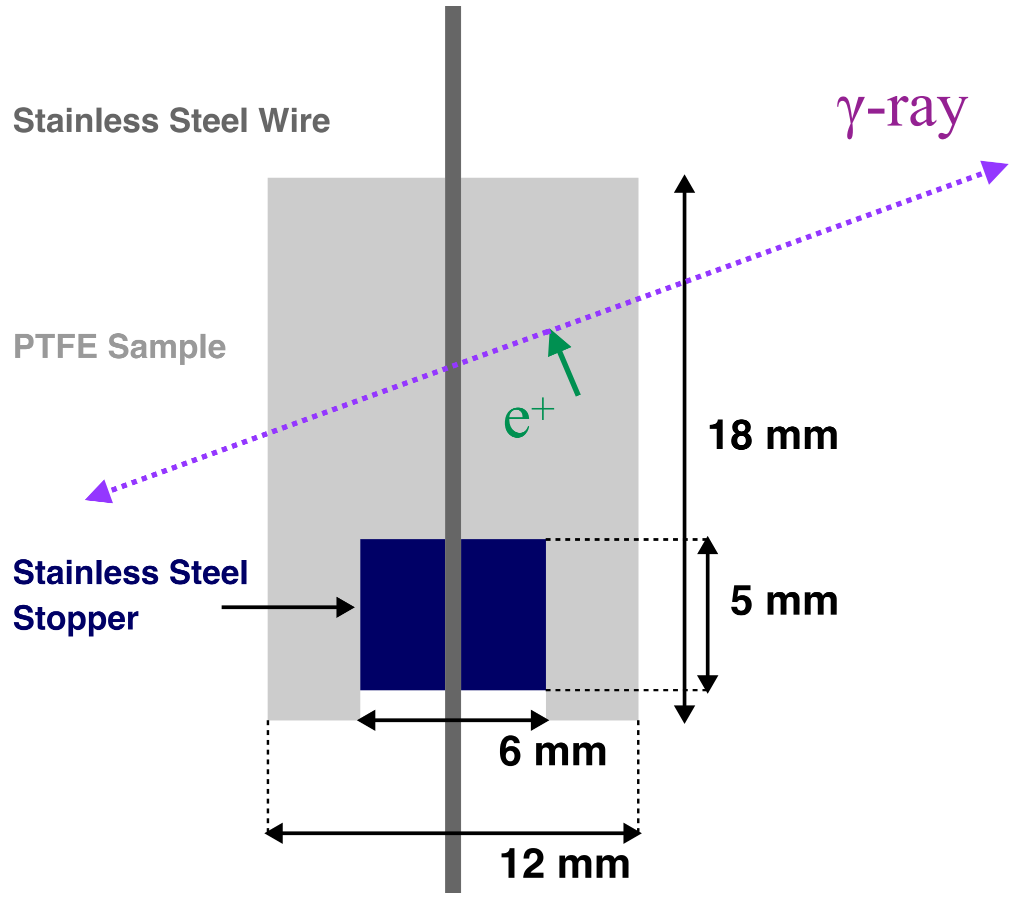

- New calibration sources are under development.
- ^{18}F (β^+-decay, $\tau_{1/2}$~110 minutes) is produced by irradiating fast-neutrons into PTFE (C_2F_4), $^{19}F(n, 2n)^{18}F$.
- Two 511 keV γ-rays from the e^+ annihilation within the PTFE volume will serve as a useful calibration source (replacement of ^{68}Ge).
- Conducted laboratory scale tests with a D-T neutron generator.

New Calibration Sources (2)

PoS ICRC2023, 1585 (2023)

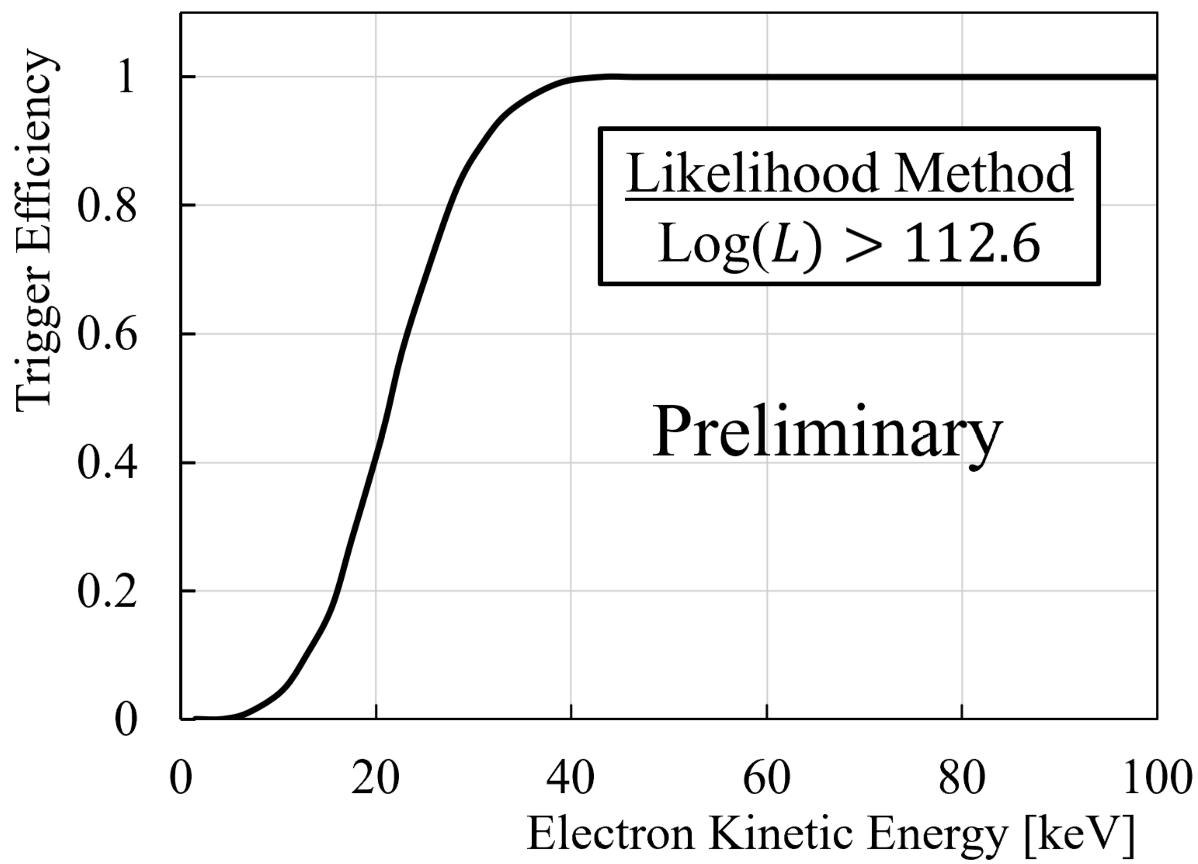

γ-ray Energy Spectrum
Taken by a High Purity Germanium detector

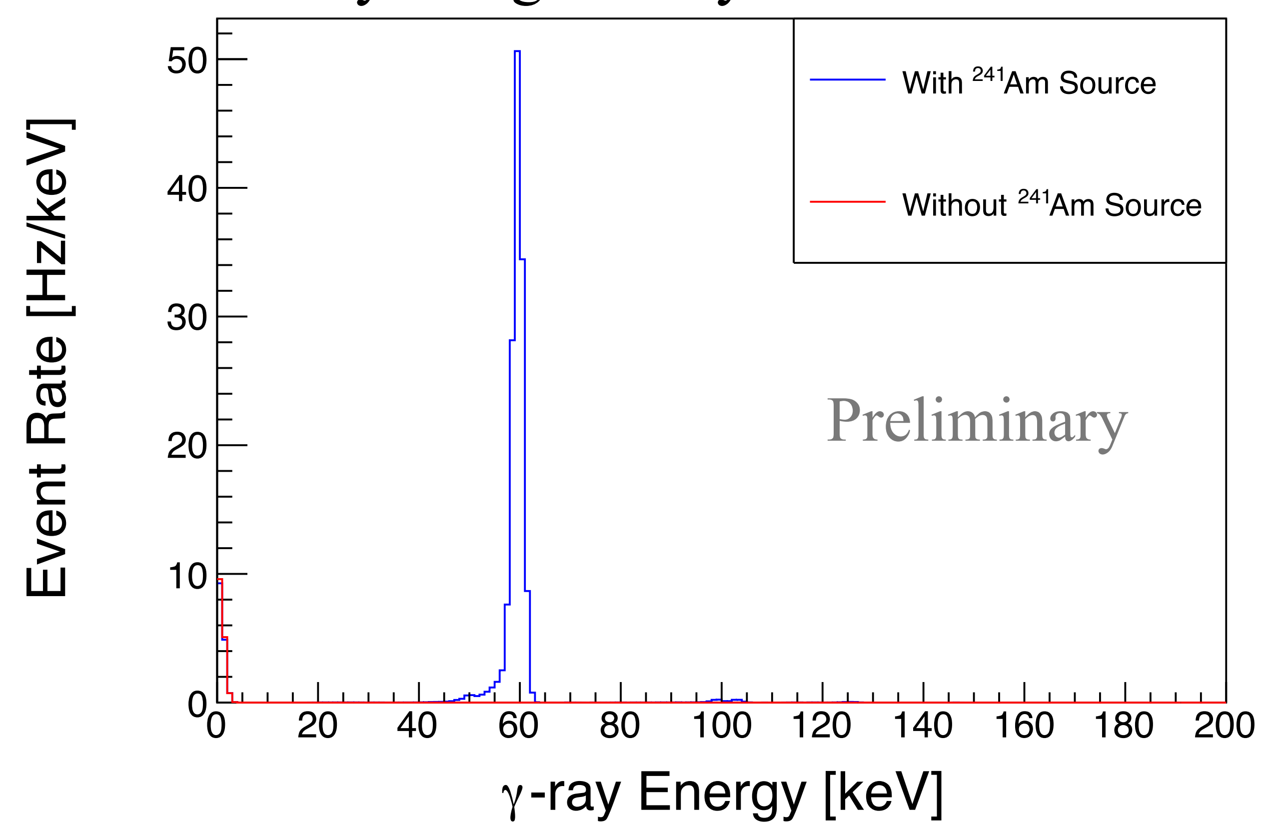

- A new trigger system, capable of lowering the energy threshold to ~20 keV, has been developed to maximize the astrophysics potential.
- Following this development, low-energy calibration sources are prepared. PoS TAUP2023, 289 (2024)
- An ^{241}Am source, emitting a ~59.5 keV γ-ray after its α-decay, has been prepared to cover this lowest energy region in JUNO.

Summary

- Overviewed the calibration programs in the JUNO experiment.
- JUNO aims to determine the neutrino mass ordering by achieving:
  - an optimal energy resolution of 3% at 1 MeV, and
  - better than 1% systematic uncertainty on the energy scale.
- Various calibration plans have been established:
  - Several radioactive calibration sources to understand the non-linearity of the LS light yield.
  - Four different calibration source deployment systems to correct the position-dependent energy scale.
  - Calibration of the 20-inch PMT response using the laser system.
- In addition, new calibration sources are under development, such as ^{18}F, and low-energy calibration sources.
  - Paper about these new calibration sources is in preparation.

Backup

Energy Calibration

$$f_{\text{non-linear}} = \frac{E^{\text{e}}_{\text{vis}}}{E^{\text{e}}}$$

$$f_{\text{non-linear}} = \frac{p_0 + p_3/E^{\text{e}}}{1 + p_1 \text{e}^{-p_2 E^{\text{e}}}}$$

$$E^{\gamma}_{\text{vis}} = \int_0^{\text{E}^{\gamma}} P(E^{\text{e}}) \times f_{\text{non-linear}}(E^{\text{e}}) \times E^{\text{e}} dE^{\text{e}}$$

E_{e} : Electron/positron kinetic energy.

E_{vis} : Visible energy.

$P(E^{\text{e}})$: Probability density function of electron/positron emission with a kinetic energy of E^{e} from a given γ-ray source.

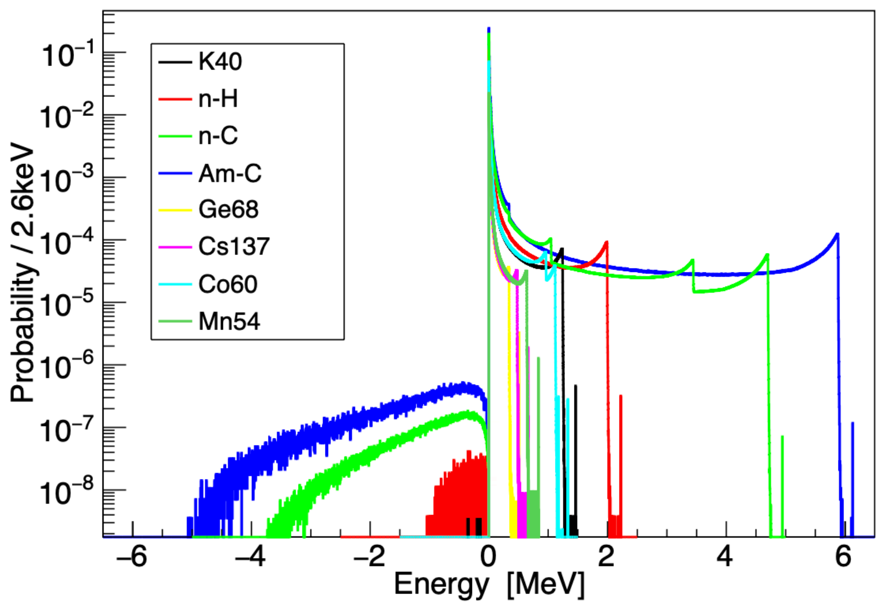

Figure 4–4 The probability density function (PDF) for primary electron of gamma from the calibration source. The parts with energy less than 0 are corresponding to the events with positron annihilation in flight. The annihilation in flight means that not all the kinetic energy of positron converts into the scintillation light, which should be subtracted in the PDF.

^{12}B Energy Distribution

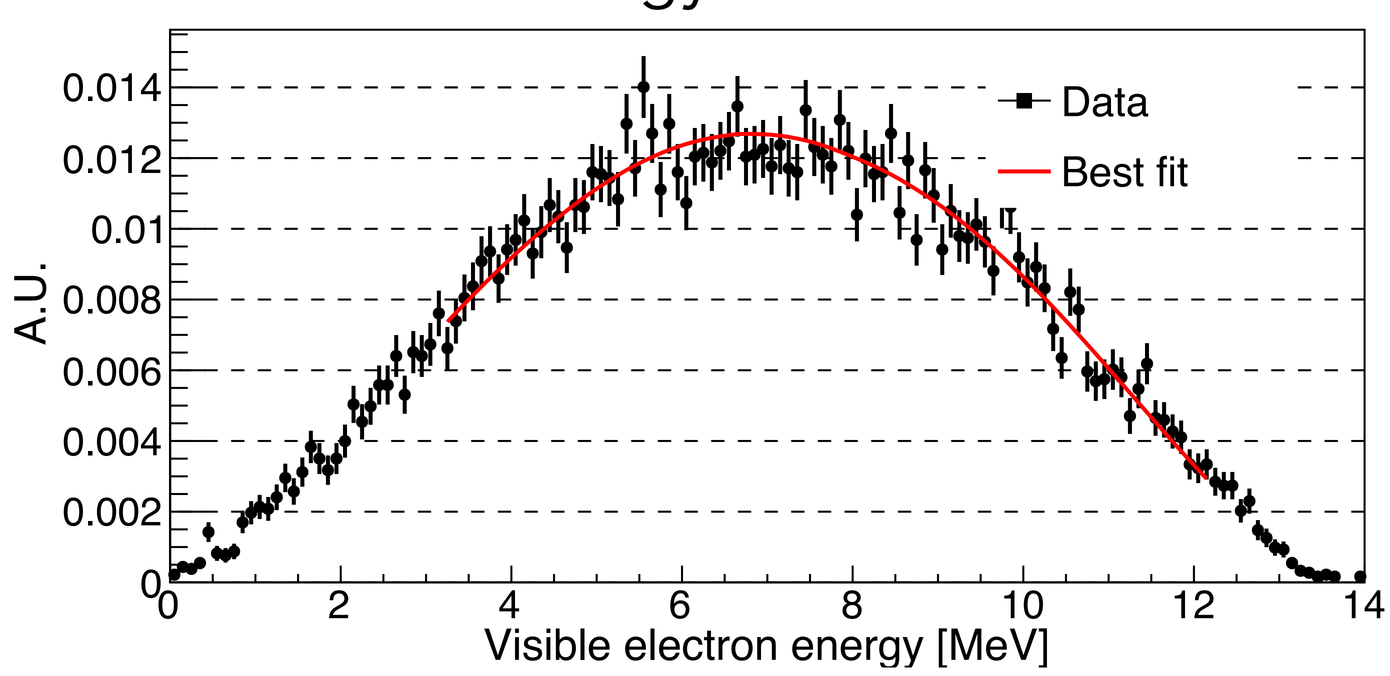

Calibration of PMT Response

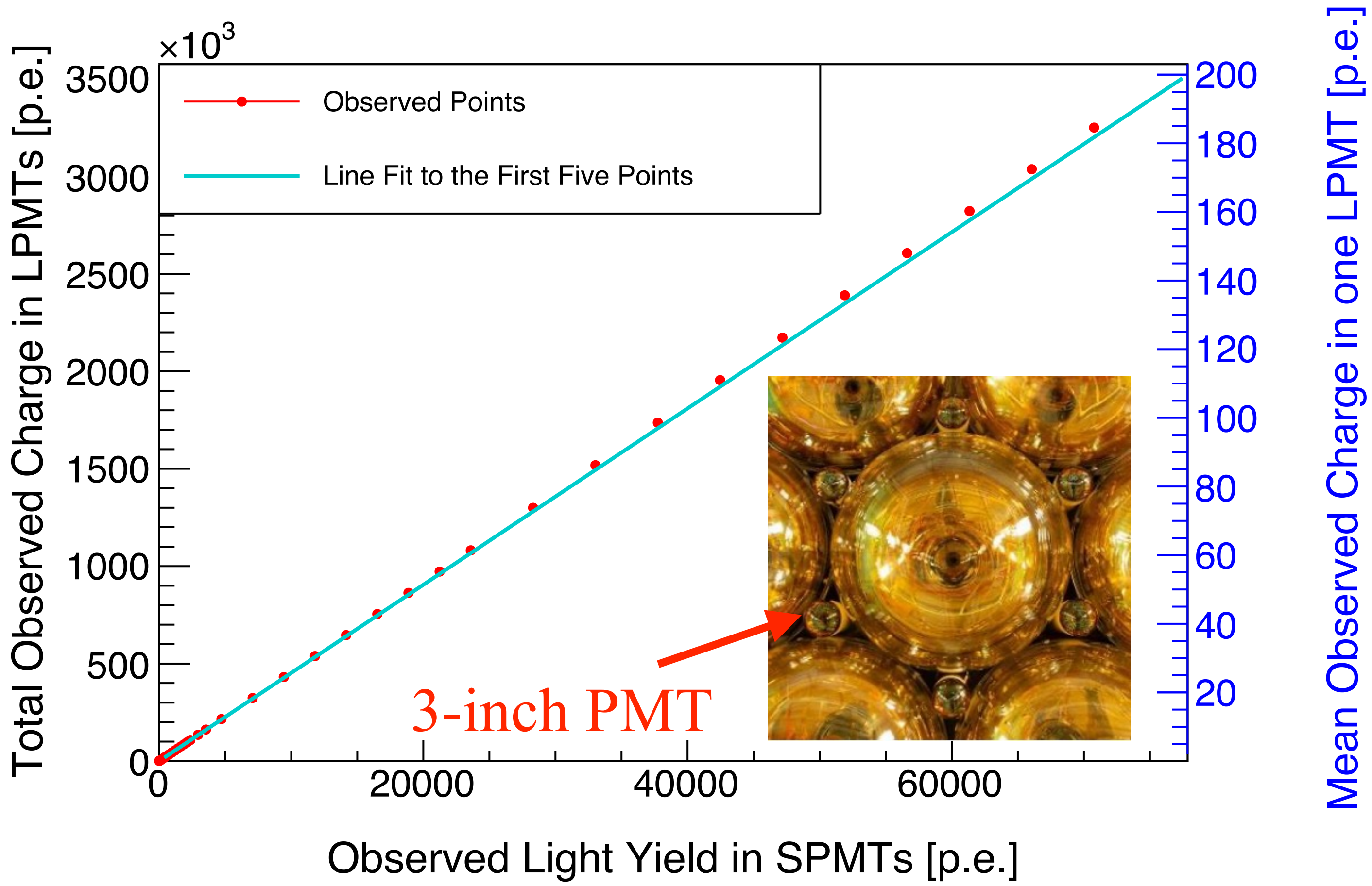

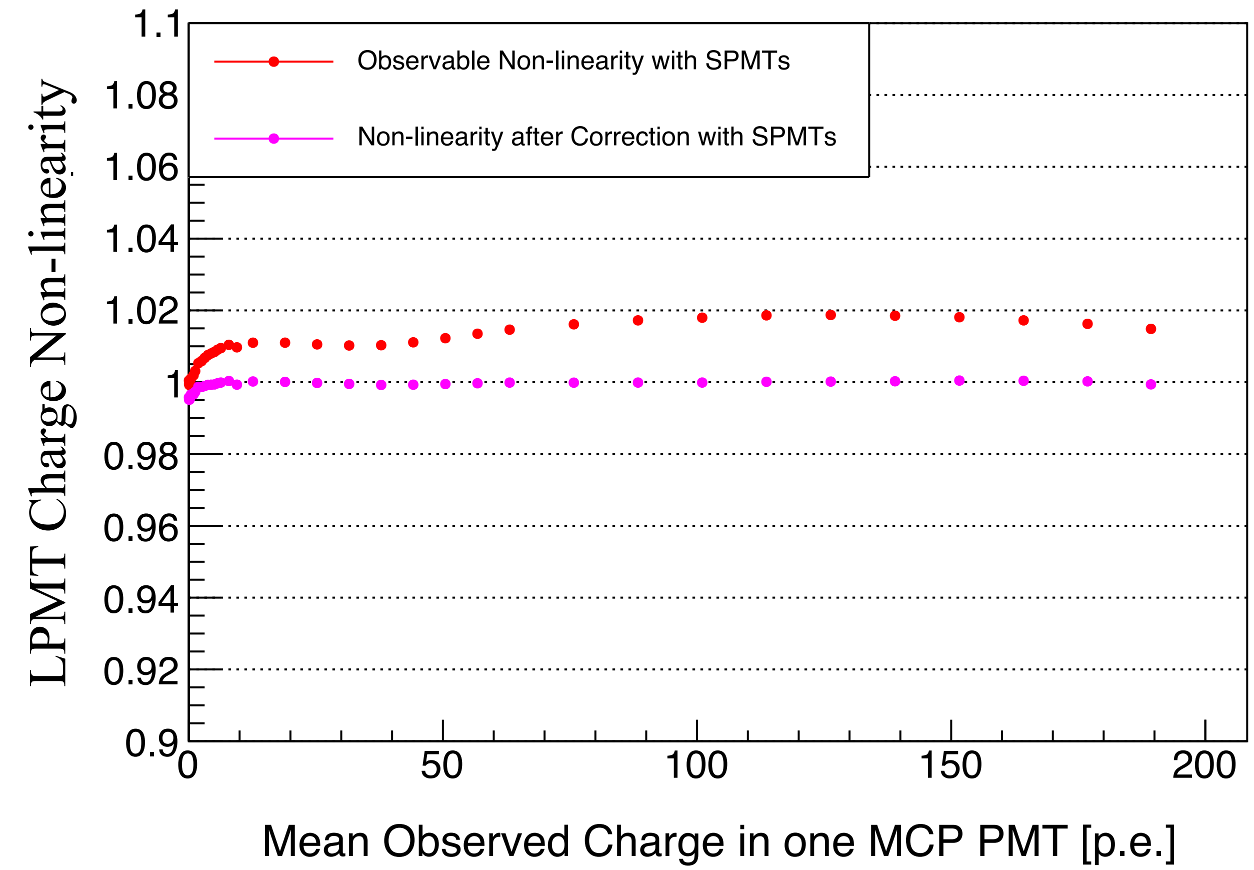

- The non-linearity of the charge response in individual 20-inch PMTs (LPMTs) is also the key to the precise energy measurement.
- This calibration is done by illuminating laser photons of various intensities and monitoring the LPMT charge response with the 3-inch small PMTs.
- The 3-inch PMT response can be regarded as a linear reference due to its small acceptance.

Treatment of SPMTs

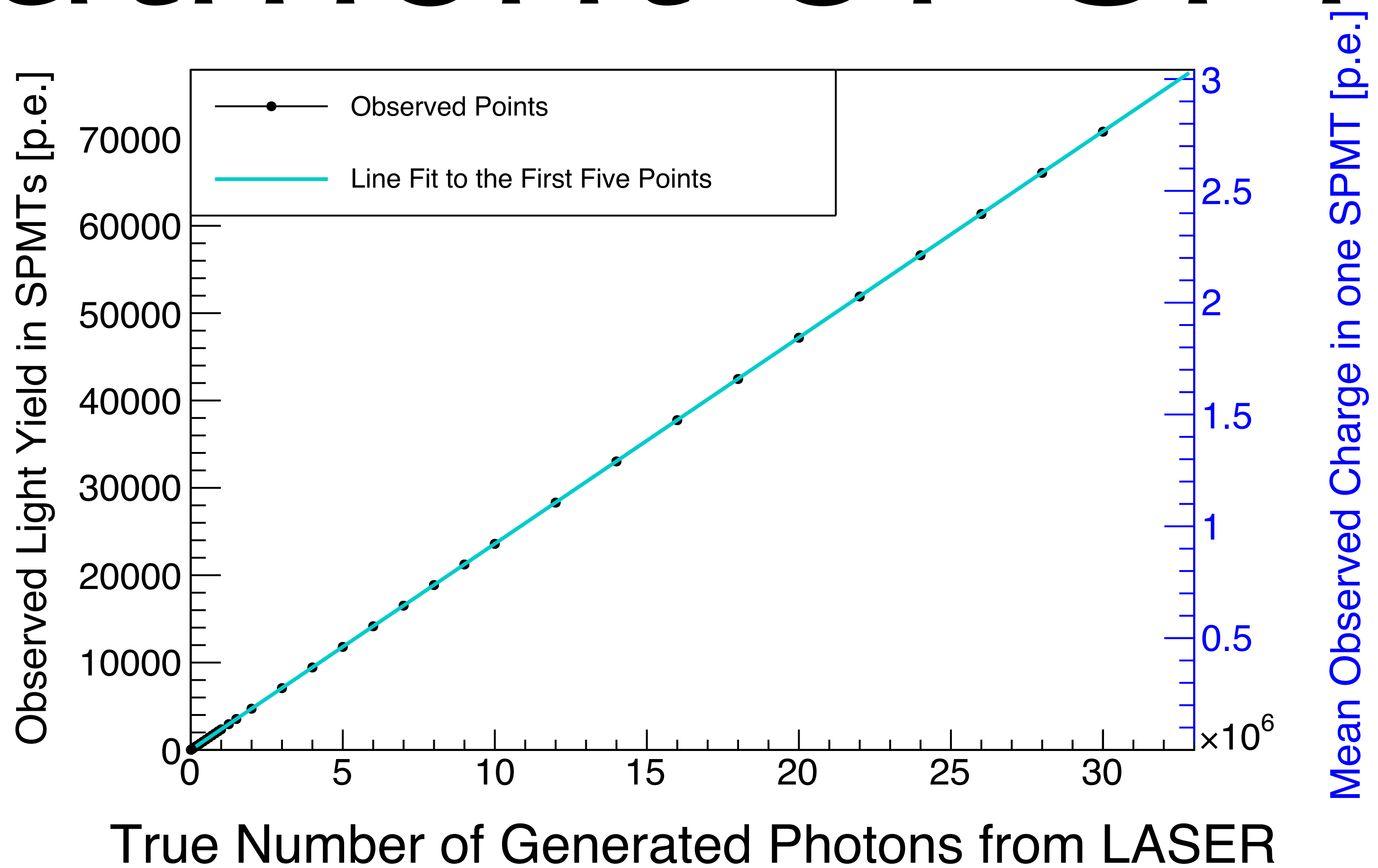

$$
\begin{aligned}
(\text{Unhit Probability}) &= \text{Poisson}(0, \mu) \\
&= \exp(-\mu) \\
&= \frac{N_{\text{total}} - N_{\text{hit}}}{N_{\text{total}}},
\end{aligned}
$$

$$
\mu = -\log\left(\frac{N_{\text{total}} - N_{\text{hit}}}{N_{\text{total}}}\right),
$$

$$
(\text{Observed Light Yield in SPMTs}) = \sum_{i}^{\text{SPMTs}} \mu_i .
$$

Energy Resolution

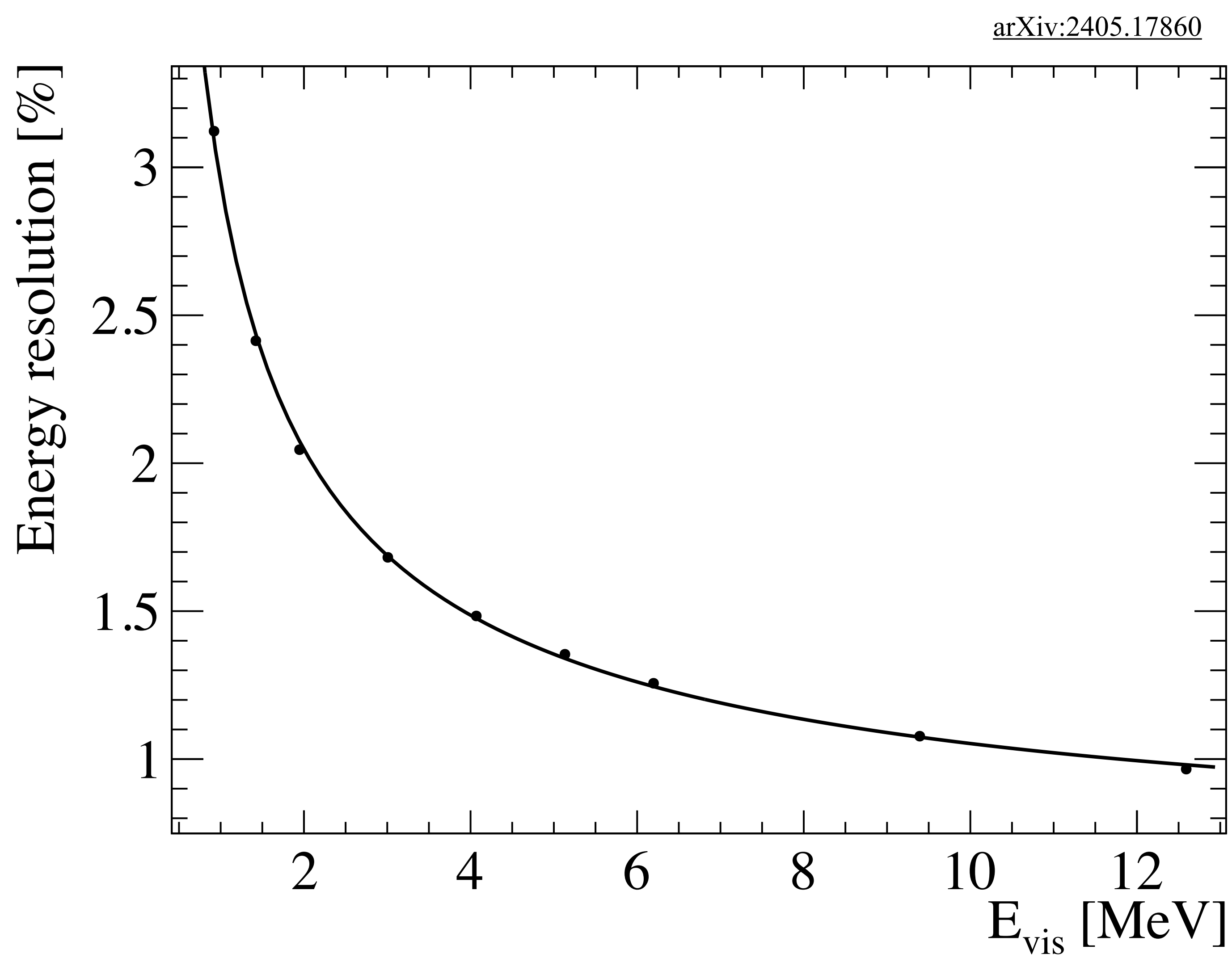

- The energy resolution curve after the event reconstruction.
- The reconstruction removes the detector non-uniformity.
- The energy resolution at E_{vis} = 1 MeV is 2.95%.

Expected Energy Spectrum

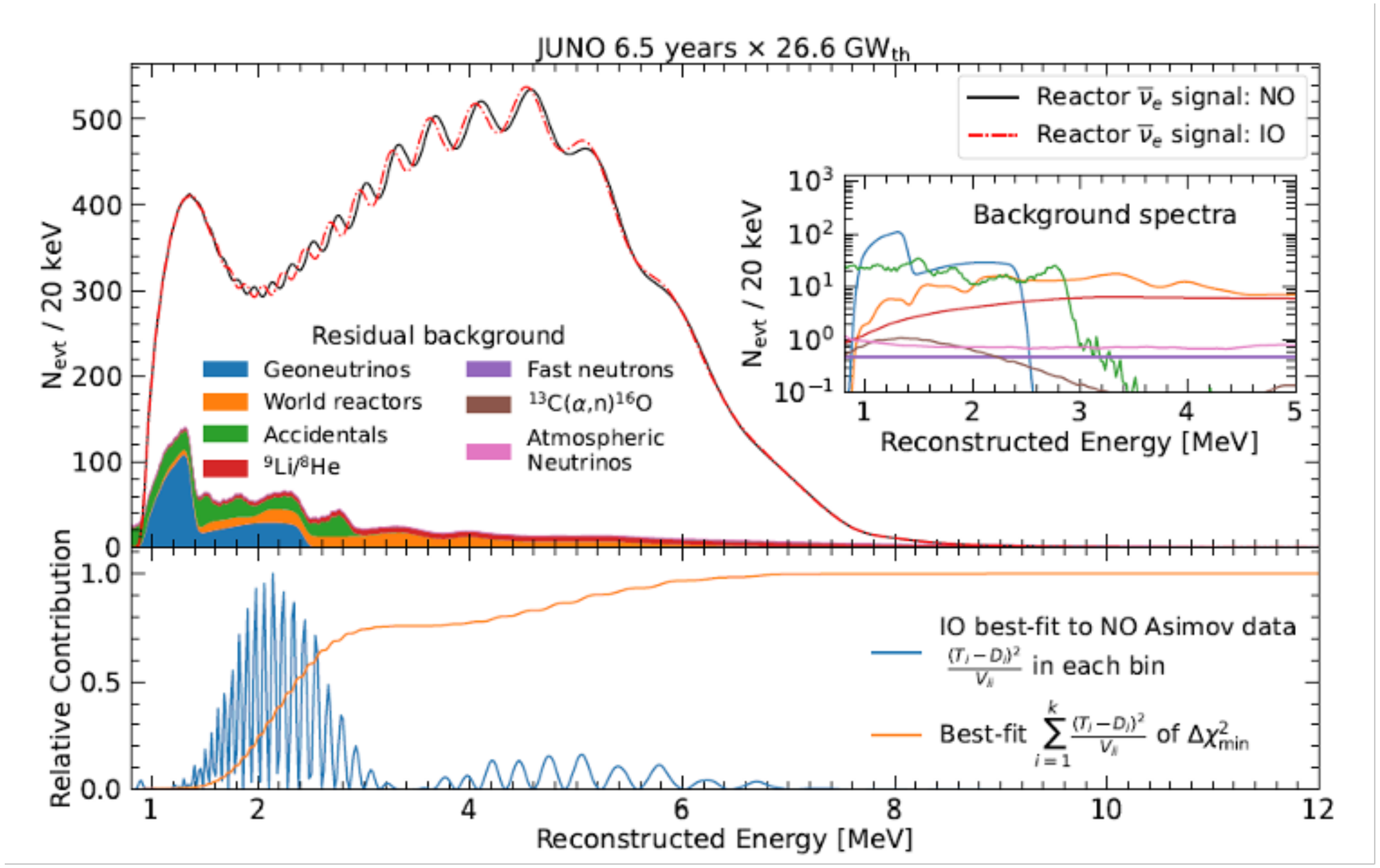

Calibration House

Energy Threshold of Isotope Production

Table 1. Nuclear reaction energies Q (in MeV) and products (with their half-lives) of the 14 MeV neutron induced reactions of ^{19}F, $^{12,13}C$ and $^{14,15}N$ isotopes.

Reaction		$_6C$		$_7N$	
	$^{19}_{9}F$ 100%	$^{12}_{6}C$ 98.89%	$^{13}_{6}C$ 1.11%	$^{14}_{7}N$ 99.64%	$^{15}_{7}N$ 0.36%
(n,2n)	$^{18}_{9}F$ -10.4 109.7 min β^+ 96.9% EC 3.1%	$^{11}_{6}C$ -18.7 20.4 min β^+ 99.76% EC 0.24%	$^{12}_{6}C$ -4.45 stable	$^{13}_{7}N$ -10.6 9.96 min β^+ 100%	$^{14}_{7}N$ -10.8 stable
(n,p)	$^{19}_{8}O$ -4.0 26.9 s β^-	$^{12}_{5}B$ -12.6 0.02 s β^-	$^{13}_{5}B$ -12.7 0.017 s β^-	$^{14}_{6}C$ 0.6 5730 y β^-	$^{15}_{6}C$ -9.0 2.45 s β^-
(n,α)	$^{16}_{7}N$ -1.5 7.1 s β^-, γ	$^{9}_{4}Be$ -5.7 stable	$^{10}_{4}Be$ -3.8 16×106 y β^-	$^{11}_{5}B$ -0.2 stable	$^{12}_{5}B$ -7.5 0.02 s β^-, γ
(n,pn) (n,d)*	$^{18}_{8}O$ -8.0 -5.0 stable	$^{11}_{5}B$ -16.0 -13.8 stable	$^{12}_{5}B$ -17.5 -15.3 0.02 s β^-, γ	$^{13}_{6}C$ -7.6 -5.3 stable	$^{14}_{6}C$ -10.2 -8.0 5730 y β^-

*Q(n,d) = Q(n,np) + 2.22 MeV